Improving the Detection of Near Earth Objects for Ground Based Telescopes

Anthony O'Dell
Captain, United States Air Force
Air Force Research Laboratories

ABSTRACT

Congress has mandated the detection of 90 percent of 140 meter diameter and larger Near Earth Objects (NEOs). While a dedicated satellite would be the preferred method of detection, ground-based telescopes are the current detection technology available. With current detection techniques, 140 meter diameter NEOs at 1 astronomical unit or more away from Earth are difficult to detect. In order to increase their detection, the methods of data collection and data analysis must be addressed.

Detection of NEOs, to include but not limited to asteroids, comets, and satellites, using ground-based telescopes with Nyquist sampling and a matched filter for point source objects are investigated as a image processing method to increase detection rates. Computer simulations for a 1 meter diameter telescope with a 128-by-128 charge coupled device (CCD), one second integration, and a 20.7 visual magnitude point source object within the CCD field of view (FOV) were computed using MatLab code. The simulation results for Nyquist sampling with cross-correlation of a point spread function (PSF) and a threshold detector are compared to Rayleigh sampling with a threshold detector. For accurate PSF calculations, atmospheric seeing measurements at the time of data collection are necessary, so various atmosphere seeing values, from 10 cm to 20 cm, are simulated and compared. Nyquist sampling with PSF cross-correlation and a threshold detector is found to be an improvement over Rayleigh sampling with a threshold detector for atmospheric seeing parameters of 10 cm to 20 cm for all simulations. The improvement over Rayleigh sampling is increased as the atmospheric seeing becomes worse. The affects of incorrect measurement of the seeing parameter are also simulated and analyzed.

Simulations for the NEO in varying locations within the CCD pixel FOV are computed and analyzed. Nyquist sampling with PSF cross-correlation is an improvement over Rayleigh sampling for all locations with the improvement increasing as distance from the CCD FOV center is increased.

Computer simulations show that Nyquist sampling with PSF cross-correlation outperforms Rayleigh sampling regardless of position within the CCD pixel FOV and for all atmospheric seeing parameters between 10 and 20 cm in detection of point source objects at a telescopes limiting visual magnitude.

INTRODUCTION

Near Earth Objects (NEOs) have been a hazard for Earth and our satellites which we have become dependant. This danger brought the U.S. Congress to mandate the detection of 90% of NEOs 140 meters and larger to be discovered and cataloged by 2020 [1]. To achieve this objective, large sky scans have begun from ground-based telescopes in both hemispheres. Current resources do not allow for the completion of the mandate by 2020 and funds are not available for dedicated space-based telescopes [1]. To improve the detection probability, a new image process is discussed in this paper for point sources which NEOs are a subset.

Limited space-based telescopes require the use of ground-based telescopes to detect or track several types of point source objects in the sky. Point source objects range from satellites, space debris, asteroids, comets, and more. Many of these point source objects are at or beyond the limiting visual magnitudes of the ground-based telescopes. Costly larger telescopes at higher altitudes are one way to attack the problem. A less costly approach is the use of existing telescopes, but improving the spatial sampling rate by using newer charge coupled device (CCD) technology and filtering the images using a point spread function, (PSF).

The improved CCD image allows for the sampling rate to be increased to Nyquist which will be shown to improve point source object detections by allowing for filtering using the PSF. The filtering is accomplished by cross-correlating the image with a calculated PSF for the limiting visual magnitude point source object. The PSF is calculated by measuring the atmospheric turbulence at the time of data collection

along with the aperture size, integration time, and limiting visual magnitude of the telescope at that integration time.

Increasing the spatial sampling rate allows for the PSF to be more well defined in the image. This improvement results in the PSF retaining its shape regardless of where the point source is in the pixel reference frame. This spatial invariance allows the use of cross-correlation to depress the background noise while keeping the point source signal intact and therefore result in a greater detection probability from a threshold detector.

Computer simulations in MatLab are used to explore the application of this process to the search for point sources versus the use of Rayleigh sampling with just a threshold detector.

METHODOLOGY

The process requires the understanding of the PSF created by atmospheric turbulence, the necessity of improved spatial sampling, and cross-correlation which are detailed below.

Atmospheric turbulence results in photons from a NEO point source spreading out as they travel though the atmosphere. The spreading of photons results in a PSF. The PSF can be used as a filter if it is spatially invariant.

The mathematical representation of the optical transfer function (OTF) which is the two dimensional Fourier transform of the PSF for ground-based optical telescopes is given in equation (1). r_0 is the atmospheric seeing parameter, ν is the spatial frequency variable, f is the focal length of the telescope forming the image onto the CCD array, and λ is the wavelength of the light being observed by the telescope [2].

$$OTF(\upsilon) = e^{-3.44(\frac{\lambda f \upsilon}{r_0})^{\frac{5}{3}}} \tag{1}$$

Equation (1) is referred to as the long OTF. The integration times for all simulations are much greater than .001 seconds and therefore fall in the range of the long OTF [2].

Most sky scans from ground-based telescopes currently use Rayleigh sampling with a threshold detector. This technique allows for most of the photons from the point source to be collected in one pixel unless the point source is near the edge of the CCD pixel.

Rayleigh sampling is the empirical diffraction limit of a lens to differentiate between two point sources [2]. The diffraction is caused by the light traveling through the lens which acts as a single slit. This sampling limit is given by equation (2) where D is the lens diameter in meters, λ is the wavelength of light in meters, and θ is the angular resolution.

$$\theta = \frac{1.22\lambda}{D} \tag{2}$$

Rayleigh sampling is the limiting resolution possible by the human eye, but with computer image processing that is not necessarily the case. Rayleigh sampling is subjective and therefore not necessarily a complete description of the image [2].

Fig. 1. shows the simulated shape of a 21.7 visual magnitude point source in the center of a pixel's field of view (FOV) of a 128-by-128 CCD for a one meter telescope with a one second integration and Rayleigh sampling. Fig. 2. shows the simulated shape of the 21.7 visual magnitude point source in the corner of a pixel's field of view (FOV) of a 128-by-128 CCD for a one meter telescope with a one second integration and Rayleigh sampling.

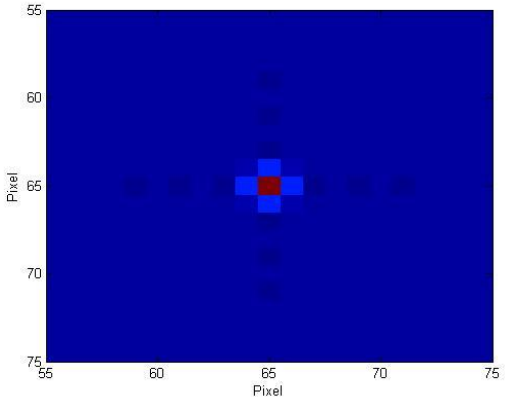

Fig. 1. Point source in center of pixel FOV, Rayleigh sampling, and r_0 = 14 cm.

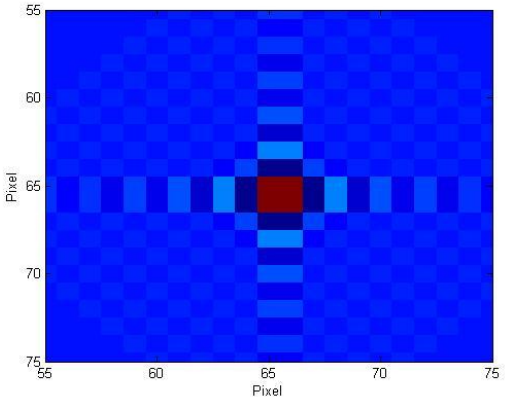

Fig. 2. Point source in corner of pixel FOV, Rayleigh sampling, and r_0 = 14 cm.

Fig. 1. shows a bright pixel adjacent to four pixels of much lower intensity. The representative shape can be described as a cross. Fig. 2. shows four bright pixels with virtually no surrounding pixels receiving any photons from the PSF resulting in a square shape. The result is a spatially variant PSF image for Rayleigh sampling of a point source object. Filtering is not applicable to a spatially variant image. Previous simulations have substantiated this claim [3].

Nyquist sampling is defined as the largest sample period that produces a digital signal from an analog signal [2]. This resolution limit is given by equation (3) where D is the lens diameter in meters, λ is the wavelength of light in meters, and θ is the angular resolution.

$$\theta = \frac{\lambda}{2D} \tag{3}$$

Using any larger sampling will result in loss of information and aliasing [4]. Using smaller sampling will not result in anymore frequency information but should more finely describe the PSF.

Fig. 3. shows the simulated shape of a 21.7 visual magnitude point source in the center of a pixel's field of view (FOV) of a 128-by-128 CCD for a one meter telescope with a one second integration and Nyquist sampling. Fig. 4. shows the simulated shape of a 21.7 visual magnitude point source in the corner of a pixel's field of view (FOV) of a 128-by-128 CCD for a one meter telescope with a one second integration and Nyquist sampling.

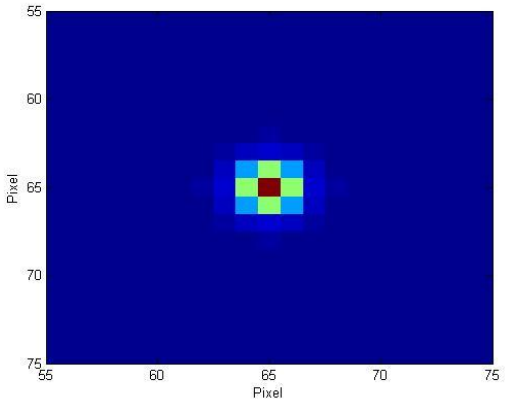

Fig. 3. Point source in center of pixel FOV, Nyquist sampling, and r_0 = 14 cm.

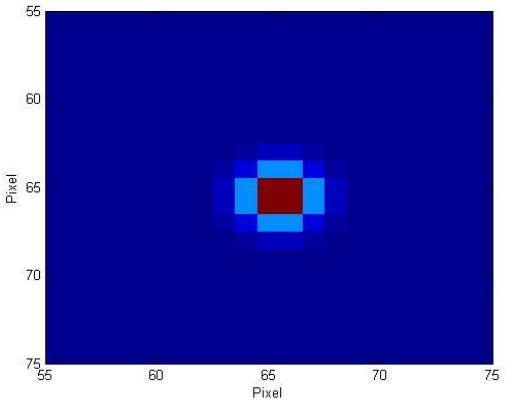

Fig. 4. Point source in corner of pixel FOV, Nyquist sampling, and r_0 = 14 cm.

Fig. 3 shows a high intensity pixel surrounded by multiple pixels that create a circular shape. Fig. 4 shows four high intensity pixels with multiple other pixels that create a circular shape. This is

representative of the ability of Nyquist sampling to retain the shape of the PSF and therefore be spatially invariant.

The spatial variance of Rayleigh sampling and spatial invariance of the Nyquist sampling is described in fig. 5.

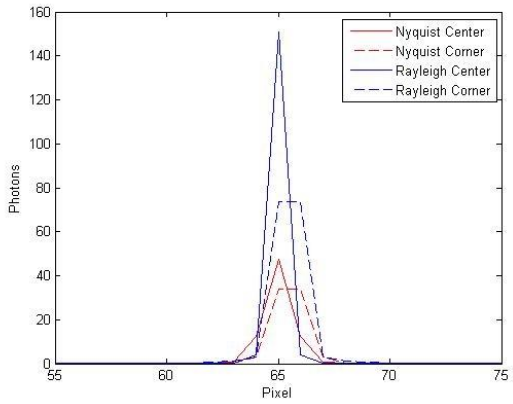

Fig. 5. Photons per pixel for Rayleigh and Nyquist sampling for r_0 = 14 cm. X-axis represents the x and y coordinate of CCD array.

Fig. 5 shows a 51 percent decrease from Rayleigh sampling with the point source in the center of the pixel FOV to Rayleigh sampling with the point source in the corner of the pixel FOV. It also shows a 26 percent decrease from Nyquist sampling with the point source in the center of the pixel FOV to Nyquist sampling with the point source in the corner of the pixel FOV. While Rayleigh sampling has a greater percentage of photons in one pixel, it also has higher background intensity per pixel and the PSF is spatially variant which does not allow for filtering. Nyquist sampling has fewer photons per pixel but also has lower background intensity per pixel and is spatially invariant which allows for filtering.

Spatial invariance allows for cross-correlation between the calculated PSF and the Nyquist sampled image.

Cross-Correlation measures the strength and direction of the linear relationship between two sets of random variables without normalizing the resulting values to between -1 and 1 [4]. In these simulations, the two sets of random variables are the values contained in the matrixes of the CCD image and the calculated PSF image.

Comparison of two sets of 2-dimensional data is defined by equation (2)

$$(fg)[b,n] = \sum_{j=-\infty}^{\infty} \sum_{m=-\infty}^{\infty} f^*[j,m]g[j+b,m+n] \tag{4}$$

where one data set, f, is multiplied by another data set, g, as g is shifted with respect to f in both dimensions.

In the frequency domain, cross-correlation is defined by equation (3) where * represents the complex conjugate [4].

$$cross-correlation \equiv FFT^{-1}\{FFT(A) \times FFT(B)^*\} \tag{5}$$

In equation (3), A and B are signals and in this particular case the CCD and PSF images. If they are similar in form, they will cross-correlate well and produce a high value. If they are dissimilar, they will produce a lower value then if they had been similar. These values from cross-correlation show how well the CCD image matches the PSF expected from a NEO or other point source formed by the telescope.

The effect of cross-correlation for a Nyquist sampled imaged with a point source present is shown in fig. 6 and 7. Fig. 6 is an uncorrelated image of a point source sampled at Nyquist. The point source is barely recognizable in the center of the image. Fig. 7 shows the same image that has been cross-correlated with a PSF that has been calculated using the telescopes limiting visual magnitude, telescope lens size, integration time, and atmospheric parameter at time of data collection. The point source is much more obvious in the center of the cross-correlated image.

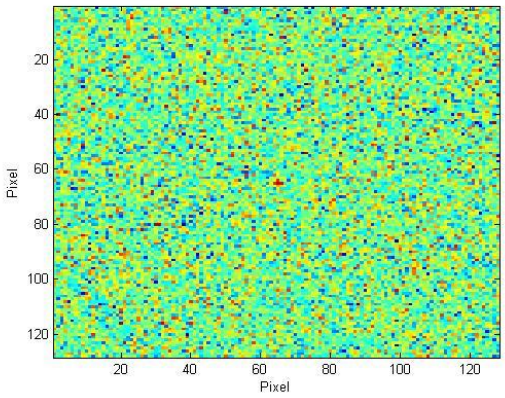

Fig. 6. Image of a point source in center of pixel (65, 65) with Nyquist sampling and r_0 = 14 cm.

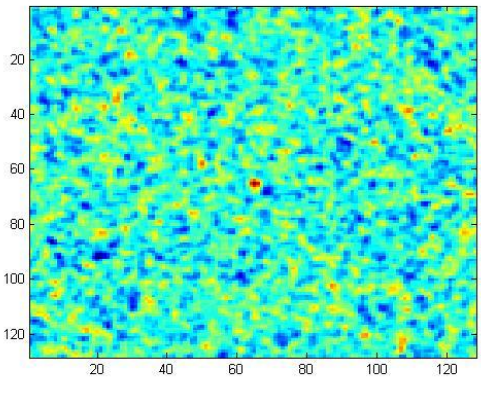

Fig. 7. Image of a point source in center of pixel with Nyquist sampling and r_0 = 14 cm. after cross-correlation with PSF.

The individual steps for this procedure are described for this paper's simulations. The telescope diameter, d, used for these simulations was 1 meter with an area of .785 square meters. An integration time of 1 second is standard for all data sets. 1000 background images and 1000 images with a NEO source present were generated for each data set for statistical purposes. The number of images was kept lower to allow faster computation.

A CCD rectangular grid with 128-by-128 pixels was used for all simulations. The size of the CCD array was limited due to computational limits available for these simulations. The quantum efficiency of the CCD is 66 percent. Also, a detection limitation of signal to noise ratio (SNR) 6 is used for all simulations.

RESULTS AND DISCUSSION

Fig. 8 and 9 shows two simulations for a NEO in the center of the pixel. The Nyquist sampling with cross-correlation of a PSF process is better than the Rayleigh sampling for all threshold values. At a threshold of 6, Nyquist detection is 2.29 times greater than Rayleigh detection.

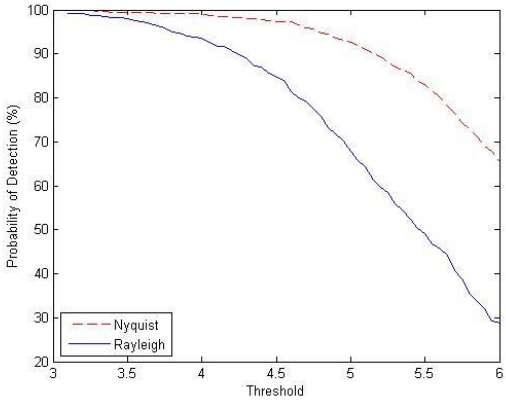

Fig. 8. Probability of detection versus threshold for a point source in center of pixel with r_0 = 14 cm.

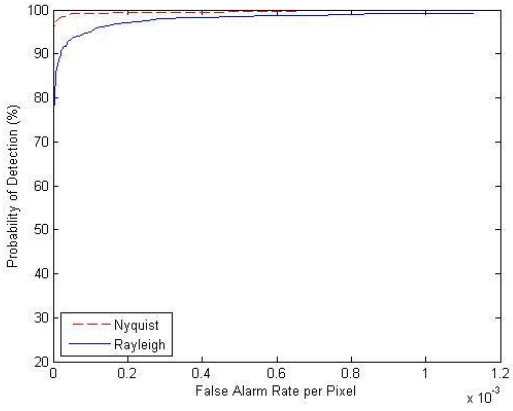

Fig. 9. Probability of detection versus false alarm rate for a point source in center of pixel with r_0 = 14 cm.

The NEO source in the center of the pixel is the best case scenario for detection probability for both Nyquist sampling with cross-correlation of a PSF and Rayleigh sampling since the maximum number of photons in any one pixel is achieved in this scenario. The cross-correlation process is most beneficial at

limiting thresholds and visual magnitudes and will allow for detection of more NEOs and specifically smaller diameter NEOs.

The Nyquist sampling with cross-correlation process is better than the Rayleigh sampling for all threshold values in fig. 10 and 11. Rayleigh sampling detection probability reduces to zero at a threshold of 6 while Nyquist sampling with cross-correlation has a detection probability of 28 percent.

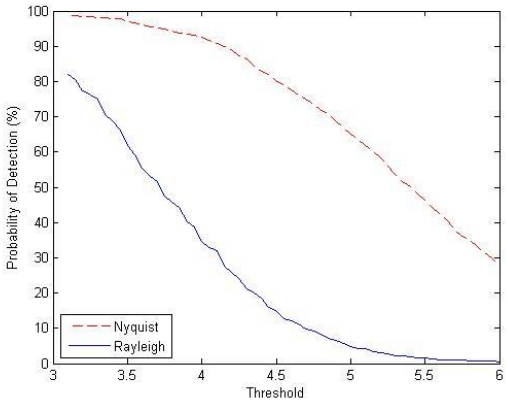

Fig. 10. Probability of detection versus threshold for a point source in corner of pixel with r_0 = 14 cm.

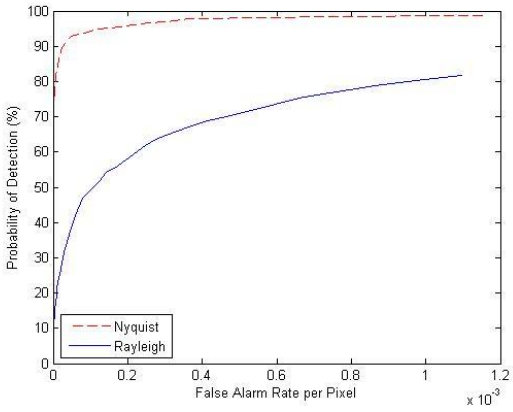

Fig. 11. Probability of detection versus false alarm rate for a point source in corner of pixel with r_0 = 14 cm.

The results from fig. 10 show the greatest improvement for Nyquist sampling with cross-correlation over Rayleigh sampling. The NEO source in the corner of the pixel is the worst case scenario for detection purposes, but may be more typical for observation since the space between pixels and the edges of pixels cover more area than center of the pixel scenarios.

Fig. 11 shows Nyquist sampling with PSF cross-correlation with a lower false alarm rate than Rayleigh sampling for all detection probabilities. This is evidence of the ability of cross-correlation to reduce the background and retain the NEO source signal.

Fig. 12 shows the trend in detection probability for both detection processes as a function of position in the FOV of the pixel. A threshold of 5 was used since the Rayleigh sampling probability of detection is almost zero before the NEO reaches the corner for a threshold of 6. A threshold of 5 allows for the divergence of the two lines to be more evident as the NEO moves closer to the corner of the pixel. As the NEO moves to the corner of the CCD pixel the detection probability of the Nyquist sampling with cross-correlation of a PSF has a nearly 30 percent drop while the Rayleigh sampling drops to almost zero. This rapid decline by Rayleigh sampling and the minimal decline of Nyquist sampling with cross-correlation of a PSF are evidence of the ability of cross-correlation to retain the NEO intensity while reducing the background in order to make NEO more detectable over Rayleigh sampling with threshold detection alone.

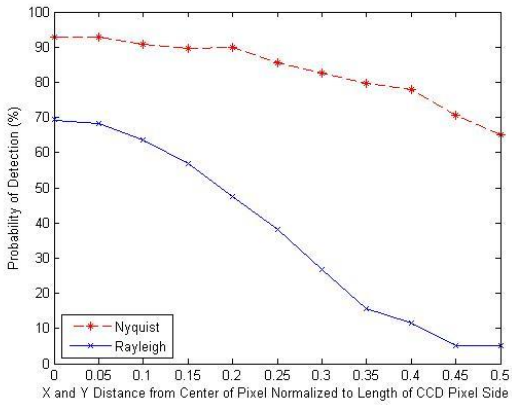

Fig. 12. Probability of detection versus position in FOV of pixel. X-axis normalized to length of each side of CCD. r_0 = 14 cm and PSF of 14 cm for a threshold of 5.

Fig. 13 shows two simulations for Nyquist with cross-correlation with a PSF of 14 cm. The detection threshold is set at 6 and the NEO source is located in the center and corner of pixel (65, 65) for the two separate simulations. The atmospheric seeing parameter is varied from 10 to 20 cm while the PSF used for cross-correlation is kept at a value of 14 cm.

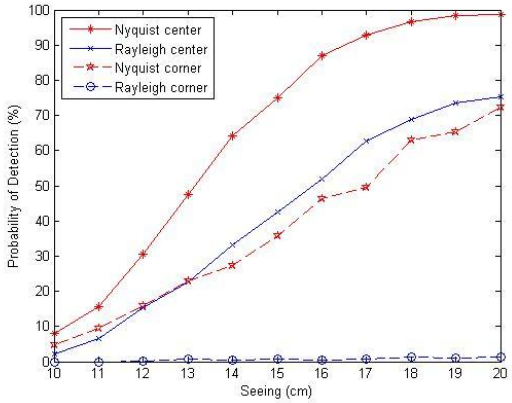

Fig. 13. Probability of detection versus seeing for a point source in corner and center of pixel with PSF = 14 cm and SNR = 6.

There is no dramatic change in the detection probability curve before or after seeing of 14 cm which infers that there is no significant loss of detection probability by incorrectly calculating the atmospheric seeing parameter for calculating the PSF. The data suggests that cross-correlation with a PSF in general is most important.

Fig. 14 shows several Nyquist with cross-correlation of PSF simulations for a NEO source in the center of the pixel with a visual magnitudes varying from 20.7 to 21.0 by increments of .1. They are for comparison purposes against a Rayleigh sampling simulation with a NEO source in the center of the pixel with a visual magnitude of 20.7. The Nyquist simulation with the closest match to the detection probability of the Rayleigh simulation is the simulation with a NEO source visual magnitude of 20.9 that is an improvement of .2 magnitude or 20.5 percent.

Fig. 15 shows simulations for an NEO in the corner of the pixel with an atmospheric seeing parameter of 14 cm. Several simulations of Nyquist sampling with cross-correlation of a PSF with varying NEO visual magnitudes were produced in order to find the best match to the Rayleigh sampling for a NEO visual magnitude of 20.7. No Nyquist simulation matched the false alarm rate of Rayleigh, but the Nyquist simulation of a NEO with a visual magnitude of 21.1 is the best match for the Rayleigh simulation with a NEO visual magnitude of 20.7 using equation (6). This would be an improvement of .4 visual magnitude which results in a 45.19 percent improvement in photon intensity.

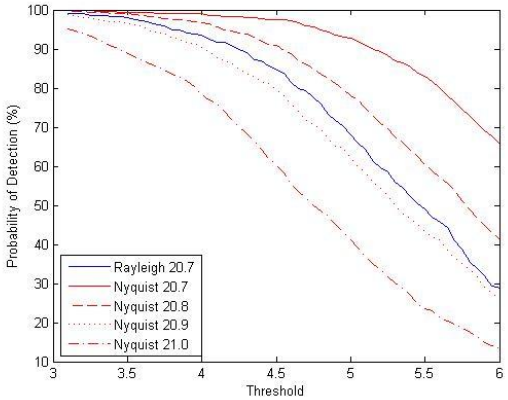

Fig. 14. Best match visual magnitude limit for Nyquist with cross-correlation to Rayleigh of visual magnitude 20.7 with a point source in center of pixel with PSF = 14 cm.

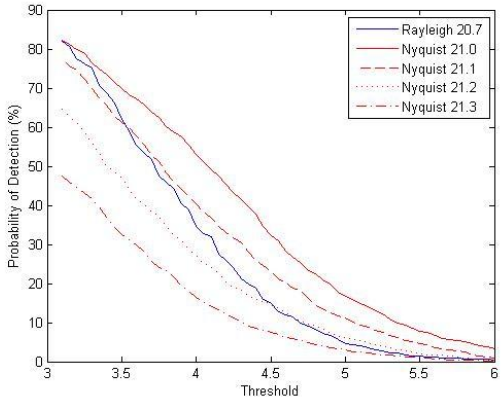

Fig. 15. Best match visual magnitude limit for Nyquist with cross-correlation to Rayleigh of visual magnitude 20.7 with a point source in corner of pixel with PSF = 14 cm.

The best match was determined using the difference between the corresponding SNR detection probabilities of the Nyquist sampling with cross-correlation of a PSF and the Rayleigh sampling, taking their absolute values and summing them which is described by equation (6) where Nyquist values are X_N and Rayleigh values are X_R.

$$\sum \left| X_N - X_R \right| \tag{6}$$

For fig. 14, the resulting values from equation (6) are 9.930 for visual magnitude 20.7, 3.964 for visual magnitude 20.8, 2.316 for visual magnitude 20.9, and 10.988 for visual magnitude 21.0.

For fig. 15, no Nyquist simulation matched the false alarm rate of Rayleigh, but the Nyquist simulation of a NEO with a visual magnitude of 21.1 is the best match for the Rayleigh simulation with a NEO visual magnitude of 20.7 using equation (6). This would be an improvement of .4 visual magnitude which results in a 45.19 percent improvement in photon intensity.

From equation (6), the Nyquist sampling of a NEO visual magnitude of 21.2 with cross-correlation of a PSF is the best match for the Rayleigh sampling of a 20.7 visual magnitude NEO in figure 22. The resulting values from equation (6) are 6.368 for visual magnitude 21.0, 2.663 for visual magnitude 21.1, 3.356 for visual magnitude 21.2, and 7.021 for visual magnitude 21.3.

When only the threshold values of 4.5 to 6 are considered, the resulting values from equation (6) are 2.776 for visual magnitude 21.0, 1.323 for visual magnitude 21.1, .222 for visual magnitude 21.2, and .526 for visual magnitude 21.3. The Nyquist simulation of a NEO with a visual magnitude of 21.2 is the best match for the Rayleigh simulation with a NEO visual magnitude of 20.7 using equation (6) for threshold values of 4.5 to 6. This would be an improvement of .5 visual magnitude which results in a 59.37 percent improvement in photon intensity.

CONCLUSION

Congress has mandated the detection of 90 percent of NEOs over 140 meters in diameter by 2020. Current assets will only allow for 90 percent detection of 1 kilometer or larger NEOs [1]. Smaller NEOs will require new detection techniques using ground-based telescopes.

The use of Nyquist sampling with cross-correlation of a PSF for large sky scan detections of NEOs increases the probability of detection over Rayleigh sampling for all positions of the point source within the pixel FOV. The improvement increases as the point source location is closer to the corner of the pixel. At SNR 6, the improvement for the NEO in the center of the pixel FOV is 129 percent and when the NEO is in the corner of the pixel FOV the probability of detection increases from 0 to 28 percent.

This process is an improvement for all atmospheric parameters between 10 and 20 cm while it provides a greater improvement over Rayleigh sampling at lower atmospheric parameters.

This improvement will not make up the shortfall in detection capability in order to reach 90 percent detection of NEOs by 2020, but it is one step closer to reaching that goal.

REFERENCES

1. Committee to Review Near-Earth Object Surveys and Hazard Mitigation Strategies, National Research Council. Near-Earth Object Surveys and Hazard Mitigation Strategies: Interim Report. August 12, 2009.
2. Goodman, Joseph W. *Goodman Statistical Optics*. John Wiley & Sons, Inc., 2000.
3. O'Dell, Anthony. Detecting Near-Earth Objects Using Cross-Correlation With a Point Spread Function. Air Force Institute of Technology, 2009.
4. Lahti, B. P. *Signal Processing and Linear Systems*. Berkeley Cambridge Press, 1998.